Proc. NIPR Symp. Antarct. Geosci., 1, 150–168, 1987

KYANITE FROM THE WESTERN PART OF THE SØR RONDANE MOUNTAINS, EAST ANTARCTICA

Masao ASAMI[1] and Kazuyuki SHIRAISHI[2]

[1]*Department of Geological Sciences, College of Liberal Arts, Okayama University, 1–1, Tsushima Naka 2-chome, Okayama 700*
[2]*National Institute of Polar Research, 9–10, Kaga 1-chome, Itabashi-ku, Tokyo 173*

Abstract: Kyanite was found in a granulite-facies pelitic gneiss from the western part of the Sør Rondane Mountains. Kyanite, accompanied by some quartz and muscovite, occurs restrictedly in biotite aggregates (Type-B biotite) by which garnet porphyroblasts are often embayed and fringed, and thus is isolated from the matrix consisting of sillimanite, tabular biotite (Type-A biotite), K-feldspar, plagioclase, quartz, ilmenite, rutile and spinel, which contacts with no quartz. The embayed garnet characteristically shows an outward X_{Fe}-increase near the embayed edge and has magnesian interior, whereas the non-embayed garnet, which is idiomorphic to hypidiomorphic and surrounded by the matrix minerals, is actually unzoned with compositions as magnesian as the former garnet interior. On the basis of the textural and paragenetic relations, it is inferred that this rock was recrystallized at two stages of metamorphism and that kyanite was formed in association with Type-B biotite, Fe-rich garnet (embayed edge), some quartz and muscovite through the retrograde reaction: garnet + K-feldspar + H_2O = kyanite + biotite + quartz. Compositions of garnet, biotite and plagioclase in addition to the mineral assemblages of the two stages suggest that the granulite-facies metamorphism has taken place at about 830°C and 8 kb followed by the kyanite-forming retrograde event under conditions of about 560°C and at least 4.5 kb.

1. Introduction

The Al_2SiO_5 minerals are important in metamorphic petrology, because their stabilities are essentially controlled by temperatures and solid pressures (*e.g.* RICHARDSON *et al.*, 1969; HOLDAWAY, 1971). One polymorph of the Al_2SiO_5 minerals has often been found together with the other one or two. It has been known that they may coexist in equilibrium with each other in one case and one or more of these Al_2SiO_5 minerals are present as metastable relics in the other case. The latter case is particularly noted not only for inferring *P-T* conditions of metamorphism but also for assessing the metamorphic history.

Granulite-facies metamorphic rocks widely occur in the western and central parts of the Sør Rondane Mountains and sillimanite is commonly found in association with K-feldspar in the rocks of pelitic composition (KOJIMA and SHIRAISHI, 1986; YAMAZAKI *et al.*, 1986; ISHIZUKA and KOJIMA, 1987; SHIRAISHI and KOJIMA, 1987). Besides such sillimanite, retrograde andalusite and cordierite are known to be developed in some pelitic rocks in the central part (YAMAZAKI *et al.*, 1986; ISHIZUKA and KOJIMA, 1987). In the course of our petrological study of the western part, we found kyanite in a

sillimanite-garnet-biotite gneiss. The mode of occurrence of kyanite in this rock is much interesting for considering its origin. The petrogenesis of kyanite would make it possible to infer the *P-T*-time path of metamorphism in this area and to compare it with those of the surrounding metamorphic regions. In this paper we will present petrographic characters of the kyanite-bearing gneiss and briefly discuss a kyanite-producing reaction and metamorphic conditions on the basis of the characters.

2. Geological Setting

Basement rocks in the western part of the Sør Rondane Mountains (71.5–72.5°S and 22.5–24.5°E) consist mainly of high-grade metamorphic rocks and plutonic rocks of various compositions. A recent geological study of this area was made in detail by KOJIMA and SHIRAISHI (1986) and SHIRAISHI and KOJIMA (1987). Only some of their results necessary for the geological setting are summarized in the following with the simplified geological map (Fig. 1).

Dominant metamorphic rocks in this area are pelitic, psammitic and intermediate gneisses, which are often accompanied by small amounts of calcareous and basic ones. It is characteristic that small masses and dikes of granite are widespread in this area. Slightly metamorphosed dolerite dikes with distinct chilled margin cut the metamorphic rocks in many places. Foliation of the metamorphic rocks strikes generally E-W and dips monoclinally southward. A shear zone trending E-W is developed in the southern portion of this area. The rocks on the northern side of the shear zone have been called Northern Group and those of the shear zone Southern Group. In the northern part of the Northern Group, the granulite-facies metamorphism is indicated by the common occurrence of mineral assemblages such as sillimanite-garnet-biotite-K-

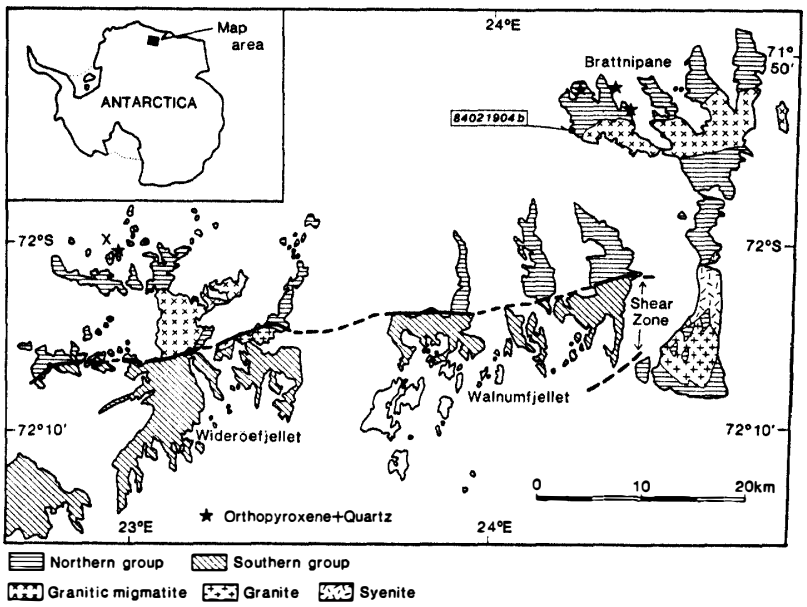

Fig. 1. Geological sketch map showing the locality of kyanite-bearing gneiss in the western part of the Sør Rondane Mountains. This is based on the geological map compiled by KOJIMA and SHIRAISHI (1986).

feldspar-plagioclase-quartz and orthopyroxene-garnet-biotite-K-feldspar-plagioclase-quartz in the pelitic to psammitic rocks and garnet-orthopyroxene-hornblende-plagioclase-quartz and two-pyroxene-garnet-hornblende-biotite-plagioclase-quartz in the basic to intermediate rocks. In the southern part of the Northern Group and in the Southern Group, on the other hand, the assemblage epidote-hornblende-plagioclase (An_{18-30}) is characteristic in the basic to intermediate rocks, suggesting the epidote-amphibolite-facies conditions. Moreover, the Southern Group is retrogressively altered by mylonitization to form epidote, chlorite and saussuritized plagioclase probably under the greenschist-facies conditions. A whole-rock K-Ar age of 536 Ma (KOJIMA and SHIRAISHI, 1986) obtained for a metadolerite dike probably indicates the time of reheating by the granite.

The kyanite-bearing gneiss (84021904B) concerned is found at an outcrop of Brattnipane in the Northern Group (Fig. 1). This rock occurs concordantly with surrounding garnet-biotite gneiss, hornblende gneiss and amphibolite.

3. Mode of Occurrence of Kyanite

The kyanite-bearing gneiss contains quartz, plagioclase, K-feldspar, biotite, garnet, sillimanite, spinel, kyanite, muscovite, rutile, ilmenite, zircon and apatite. Garnet porphyroblasts, up to 3 mm in diameter, are scattered in the gneissose matrix consisting mainly of quartz, plagioclase, K-feldspar, biotite, sillimanite, rutile and ilmenite (Fig. 2a). Spinel occurs commonly as inclusions in sillimanite, garnet and plagioclase and rarely as minute grains between plagioclase grains, so that spinel is not in direct contact with quartz. Kyanite and muscovite are isolated from such matrix minerals as K-feldspar, tabular biotite and sillimanite as described below.

Two types of biotite are distinguishable on the basis of mode of occurrence: (A) tabular crystals which form the matrix along with the felsic minerals (Fig. 2a) and most of which show parallel or subparallel alignment to the gneissosity, and (B) aggregates of randomly oriented flakes by which many garnet porphyroblasts are partially embayed and fringed (Figs. 2b and 2c). Kyanite is found restrictedly in Type-B biotite aggregates (Figs. 2c, 3a, 3b and 3c), but kyanite present near margins of the aggregates is rarely in contact with the edge of embayed garnet on one side and with plagioclase and quartz of the matrix on the other side (Fig. 3b). Minute vermicular quartz is often developed in Type-B biotite and kyanite is also in contact with such quartz (Fig. 3c). Some crystals of kyanite themselves include poikilitically minute quartz grains (Fig. 3c). No kyanite is observed in contact with some matrix minerals such as K-feldspar, sillimanite and spinel. A small amount of muscovite often occurs as fine-grained flakes in close association with Type-B biotite aggregates (Figs. 2b, 3a and 3c). Muscovite often includes vermicular quartz (Fig. 3c), and is sometimes in contact with kyanite and the embayed garnet edge and also with the matrix quartz, plagioclase and K-feldspar.

Such textural characters of the kyanite-bearing gneiss suggest that kyanite was secondarily formed replacing garnet in association with Type-B biotite, muscovite and minute quartz inclusions in Type-B biotite and kyanite. Thus, in this rock these minerals are texturally distinguishable from the primary granulite-facies minerals

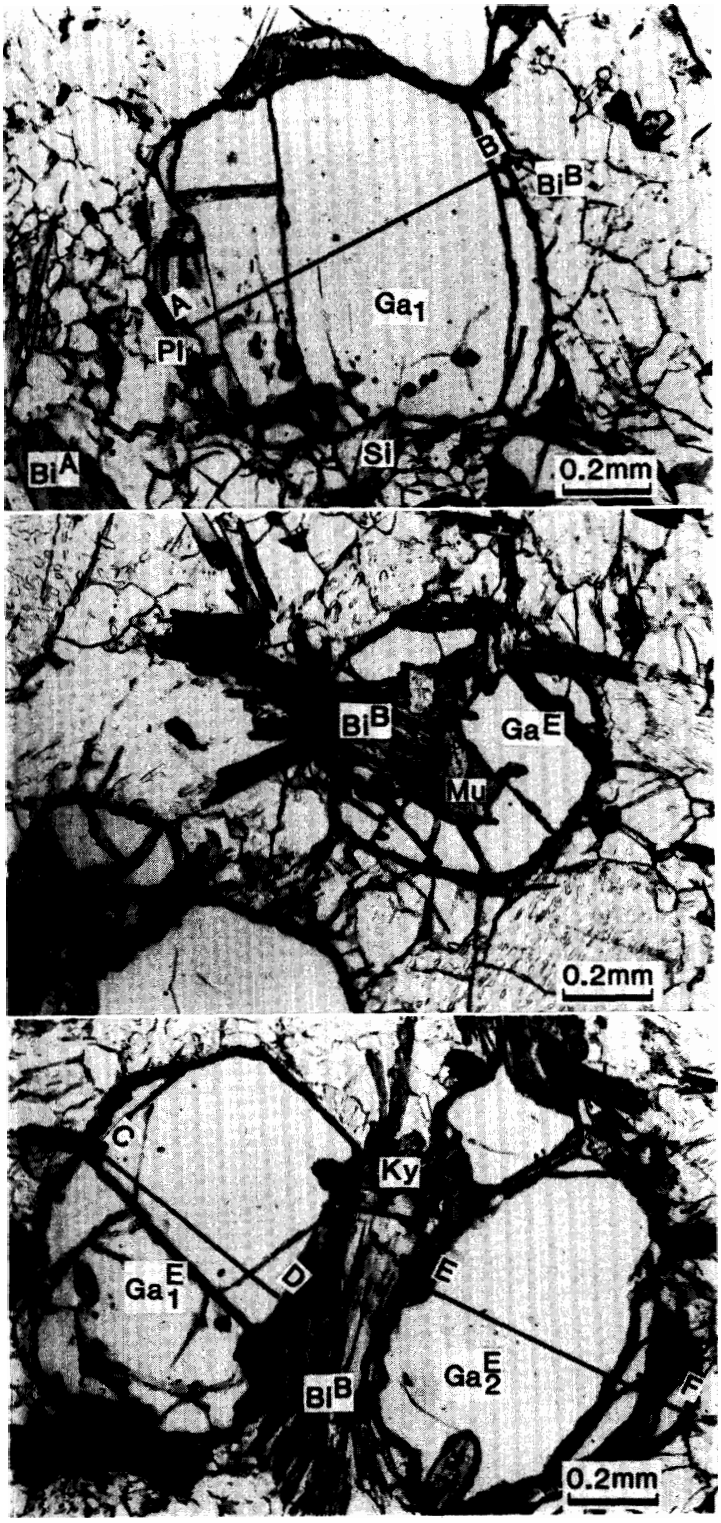

a. *A porphyroblast of non-embayed garnet (Ga_1) associated with matrix minerals such as sillimanite(Si), Type-A biotite (Bi^A), K-feldspar, plagioclase and quartz. A compositional profile shown in Fig. 5 is along the line A–B. One edge A contacts with plagioclase (Pl) and the other edge B is fringed by a minute aggregate of Type-B biotite (Bi^B).*

b. *A small porphyroblast of garnet (Ga^E) embayed by Type-B biotite (Bi^B) accompanied by muscovite (Mu).*

c. *Two porphyroblasts of embayed garnet (Ga_1^E and Ga_2^E). A small prism of kyanite (Ky) is present in an aggregate of Type-B biotite (Bi^B) developed between the porphyroblasts. Compositional profiles shown in Fig. 6 are along rhe lines C–D and E–F. The edges C, D, and E are in contact with Type-B biotite. Near the edge F adjacent to plagioclase, films of Type-B biotite are formed along rwo cracks running nearly perpendicular to the line E–F.*

Fig. 2. Photomicrographs of garnet and biotite in the kyanite-bearing gneiss (one nicol).

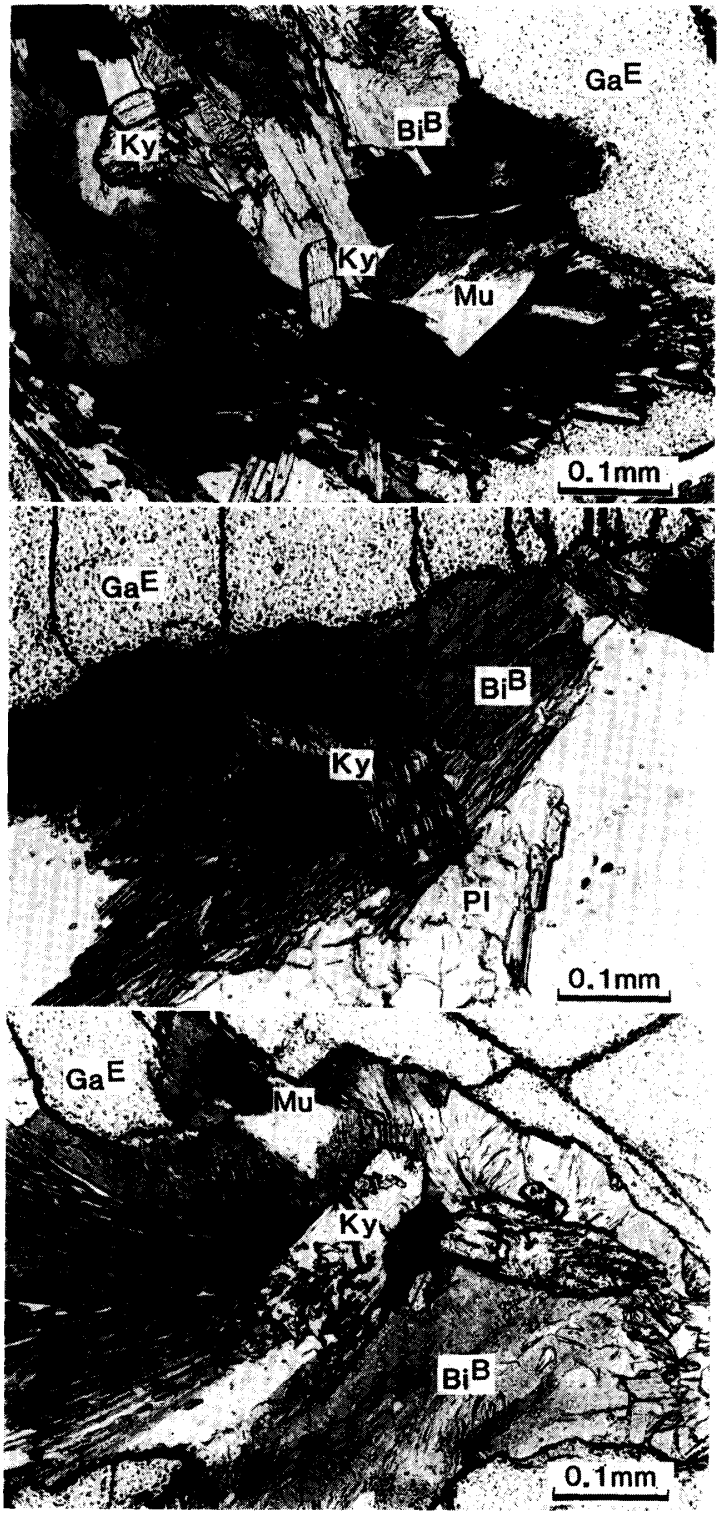

a. *Kyanite (Ky) typically developed in Type-B biotite (Bi^B) adjacent to an edge of embayed garnet (Ga^E). Muscovite (Mu) is also associated with them.*

b. *Kyanite (Ky) whose edge partially contacts with matrix plagioclase (Pl).*

c. *Kyanite (Ky) with poikilitic quartz inclusions. Also note vermicular quartz inclusions in both biotite (Bi^B) and muscovite (Mu).*

Fig. 3. Photomicrographs of kyanite in the kyanite-bearing gneiss (one nicol).

Table 1. Representative microprobe analyses of minerals in the kyanite-bearing gneiss.

	Ky	Sil	Pl_1		Pl_2		Pl_3		Kf	Sp	Il	Ru
			(C)	(R)	(C)	(R)	(C)	(R)				
No.	44	175B	179	178	157	158	130	129	28	616	428	405
SiO_2	36.90	36.91	61.68	61.56	61.08	61.61	62.40	61.99	64.23	0.03	0.05	0.02
TiO_2	0.00	0.00	0.01	0.00	0.01	0.04	0.00	0.00	0.00	0.02	53.05	99.01
Al_2O_3	62.90	61.55	23.77	23.65	23.45	23.75	23.62	23.78	18.49	59.26	0.06	0.07
Cr_2O_3	0.06	0.08	0.00	0.00	0.01	0.02	0.00	0.00	0.00	0.64	0.00	0.06
FeO*	0.26	0.17	0.07	0.08	0.00	0.24	0.00	0.12	0 03	24.20	46.31	0.54
MnO	0.00	0.00	0.03	0.00	0.00	0.00	0.04	0.03	0.09	0.01	0.33	0.00
MgO	0.03	0.04	0.01	0.00	0.00	0.00	0.00	0.00	0.00	5.99	0.10	0.00
ZnO	0.00	0.00	0.00	0.00	0.00	0.00	0.00	0.00	0.00	9.35	0.00	0.00
CaO	0.01	0.02	5.54	5.27	5.44	5.37	5.26	5.20	0.03	0.00	0.01	0.00
Na_2O	0.01	0.03	8.60	8.98	8.69	8.79	8.97	9.21	1.36	0.21	0.03	0.00
K_2O	0.01	0.00	0.11	0.18	0.14	0.23	0.15	0.17	14.79	0.01	0.01	0.01
Total	100.18	98.80	99.82	99.72	98.82	100.05	100.44	100.50	99.02	99.72	99.95	99.71
	20(O)	20(O)			32(O)		32(O)		32(O)	8(O)	6(O)	6(O)
Si	3.981	4.034	10.975	10.976	10.981	10.958	11.031	10.974	11.947	0.002	0.003	0.001
Al	7.999	7.929	4.985	4.970	4.969	4.979	4.922	4.962	4.054	3.938	0.004	0.003
Ti	0.000	0.000	0.001	0.000	0.001	0.005	0.000	0.000	0.000	0.001	2.008	2.986
Cr	0.005	0.007	0.000	0.000	0.001	0.003	0.000	0.000	0.000	0.029	0.000	0.002
Fe	0.023	0.016	0.010	0.012	0.000	0.036	0.000	0.018	0.005	1.141	1.949	0.018
Mn	0.000	0.000	0.005	0.000	0.000	0.000	0.006	0.004	0.014	0.000	0.014	0.000
Mg	0.005	0.007	0.003	0.000	0.000	0.000	0.000	0.000	0.000	0.503	0.008	0.000
Zn	0.000	0.000	0.000	0.000	0.000	0.000	0.000	0.000	0.000	0.389	0.000	0.000
Ca	0.001	0.002	1.056	1.007	1.048	1.023	0.996	0.986	0.006	0.000	0.001	0.000
Na	0.002	0.006	2.967	3.105	3.029	3.031	3.075	3.161	0.491	0.023	0.003	0.000
K	0.001	0.000	0.025	0.041	0.032	0.052	0.034	0.038	3.510	0.001	0.001	0.001
X_{Fe}										0.694		
		Or	0.6	1.0	0.8	1.3	0.8	0.9	87.6	Her 51.6		
		Ab	73.3	74.8	73.7	73.8	74.9	75.5	12.2	Spi 24.7		
		An	26.1	24.2	25.5	24.9	24.3	23.6	0.1	Gah 19.1		

Ky: kyanite, Sil: sillimanite, Pl: plagioclase, C: core, R: rim, Kf: K-feldspar, Sp: spinel, Il: ilmenite, Ru: rutile, No.: analysis number.
* Total iron as FeO. $X_{Fe}=Fe/(Fe+Mg)$.

such as garnet and the matrix minerals of Type-A biotite, sillimanite, plagioclase, K-feldspar, quartz, rutile and ilmenite. The restricted mode of occurrence of spinel in this rock suggests that spinel was stable in quartz-free domains consisting of the granulite-facies minerals except quartz and is a prograde breakdown product of any aluminous mineral which preexisted at an earlier stage of the metamorphism.

4. Mineralogy

Microprobe analyses of main constituent minerals in the kyanite-bearing gneiss were made using JXA-733 of JEOL at National Institute of Polar Research. Several grains of each mineral species and two or more points on each grain were analyzed in

Table 2. Representative microprobe analyses of garnet in the kyanite-bearing gneiss.

	Ga_1	Ga_2	Ga_2^E		Ga_3^E		Ga_4^E	Ga_5^E
	(I)	(I)	(I)	(E)	(I)	(E)	(E)	(E)
No.	185	163	120	117	66	55	40	76
SiO_2	37.97	38.35	38.25	37.60	38.32	35.95	38.19	36.78
TiO_2	0.03	0.03	0.02	0.07	0.03	0.06	0.00	0.04
Al_2O_3	22.06	21.74	21.37	21.05	21.58	20.63	20.93	20.43
Cr_2O_3	0.03	0.03	0.00	0.04	0.06	0.05	0.00	0.06
FeO*	29.22	28.76	28.65	34.08	29.80	35.84	35.08	35.75
MnO	0.70	0.61	0.68	0.88	0.70	1.28	1.40	1.51
MgO	9.51	9.25	9.20	5.24	9.22	4.79	4.26	4.03
ZnO	0.00	0.00	0.00	0.00	0.00	0.00	0.00	0.00
CaO	1.09	1.05	1.08	1.14	1.03	1.10	1.09	1.16
Na_2O	0.00	0.04	0.03	0.00	0.04	0.00	0.00	0.00
K_2O	0.00	0.00	0.02	0.01	0.00	0.00	0.00	0.03
Total	100.61	99.86	99.30	100.11	100.78	99.70	100.95	99.79
				24 (O)				
Si	5.864	5.948	5.970	5.982	5.922	5.834	6.053	5.954
Al	4.016	3.974	3.932	3.947	3.931	3.946	3.910	3.898
Ti	0.003	0.003	0.002	0.008	0.003	0.007	0.000	0.005
Cr	0.004	0.004	0.000	0.005	0.007	0.006	0.000	0.008
Fe	3.774	3.731	3.740	4.534	3.851	4.864	4.650	4.840
Mn	0.092	0.080	0.090	0.119	0.092	0.176	0.188	0.207
Mg	2.189	2.138	2.140	1.242	2.123	1.158	1.006	0.972
Zn	0.000	0.000	0.000	0.000	0.000	0.000	0.000	0.000
Ca	0.180	0.175	0.181	0.194	0.171	0.191	0.185	0.201
Na	0.000	0.012	0.009	0.000	0.012	0.000	0.000	0.000
K	0.000	0.000	0.004	0.002	0.000	0.000	0.000	0.006
X_{Fe}	0.633	0.636	0.636	0.785	0.645	0.808	0.822	0.833
Alm	60.5	60.9	60.8	74.5	61.8	76.1	77.1	77.8
Pyr	35.1	34.9	34.8	20.4	34.0	18.1	16.7	15.6
Spe	1.5	1.3	1.5	1.9	1.5	2.8	3.1	3.3
Gro	2.9	2.8	2.9	3.2	2.7	3.0	3.1	3.2

Ga: non-embayed garnet, Ga^E: garnet embayed by Type-B biotite, I: interior, E: edge. No.: analysis number.

* Total iron as FeO. $X_{Fe}=Fe/(Fe+Mg)$.

Table 3. Representative microprobe analyses of micas in the kyanite-bearing gneiss.

	Bi_1^A	Bi_2^A	Bi_3^A	Bi_4^A	Bi_2^B	Bi_3^B	Bi_4^B	Bi_5^B	Mu
No.	200	142	132	9	111	53	42	73	75
SiO_2	37.16	36.73	36.64	36.50	35.97	36.01	36.39	36.46	45.86
TiO_2	3.25	3.45	4.19	5.22	1.25	2.58	2.90	2.59	0.50
Al_2O_3	17.99	17.68	17.57	17.30	19.81	19.24	19.05	19.30	35.09
Cr_2O_3	0.03	0.07	0.09	0.11	0.03	0.00	0.09	0.00	0.00
FeO*	14.94	15.47	14.73	14.94	14.72	16.25	16.61	16.57	0.86
MnO	0.00	0.03	0.05	0.04	0.07	0.01	0.01	0.10	0.01
MgO	12.63	12.21	11.94	11.59	13.43	11.52	11.18	11.64	0.66
ZnO	0.00	0.00	0.00	0.00	0.00	0.00	0.00	0.00	0.00
CaO	0.02	0.07	0.03	0.01	0.01	0.02	0.01	0.02	0.00
Na_2O	0.05	0.05	0.05	0.11	0.11	0.11	0.10	0.10	0.38
K_2O	9.49	9.78	9.34	9.57	9.84	9.56	9.18	9.40	10.79
Total	95.56	95.54	94.63	95.39	95.24	95.30	95.52	96.18	94.15
					22 (O)				
Si	5.505	5.478	5.485	5.441	5.359	5.393	5.429	5.407	6.172
Al	3.142	3.108	3.101	3.040	3.479	3.396	3.350	3.374	5.566
Ti	0.362	0.387	0.472	0.585	0.140	0.291	0.325	0.289	0.051
Cr	0.004	0.008	0.011	0.013	0.004	0.000	0.011	0.000	0.000
Fe	1.851	1.930	1.844	1.862	1.834	2.035	2.073	2.055	0.097
Mn	0.000	0.004	0.006	0.005	0.009	0.001	0.001	0.013	0.001
Mg	2.789	2.714	2.664	2.575	2.982	2.571	2.486	2.573	0.132
Zn	0.000	0.000	0.000	0.000	0.000	0.000	0.000	0.000	0.000
Ca	0.003	0.011	0.005	0.002	0.002	0.003	0.002	0.003	0.000
Na	0.014	0.014	0.015	0.032	0.032	0.032	0.029	0.029	0.099
K	1.794	1.861	1.784	1.820	1.870	1.826	1.747	1.779	1.853
X_{Fe}	0.399	0.416	0.409	0.420	0.381	0.442	0.455	0.444	0.422
Pa									5.1

Bi^A: Type-A biotite, Bi^B: Type-B biotite. No.: analysis number.
* Total iron as FeO. $X_{Fe}=Fe/(Fe+Mg)$. $Pa=100\ Na/(K+Na)$.

general. The representative analytical data are given in Tables 1 to 3. Kyanite in this rock was optically examined on the 5-axis universal stage with the hemisphere of $n=1.649$.

4.1. Kyanite

Kyanite is fine-grained, idiomorphic to hypidiomorphic, short-prismatic crystals. In this rock some sillimanite prisms seemingly resemble kyanite, but kyanite is distinctly identified by two cleavages obliquely intersected with each other, optic orientations relative to the cleavages and optic axial angles ($2V_x=81$–$82°$, which were corrected as $\beta_{ky}=1.722$) as shown in Fig. 4. The contents of total iron as FeO are as much low as 0.2–0.4 wt% among eight kyanite grains analyzed (Table 1), so that kyanite in this rock approximates to pure Al_2SiO_5.

4.2. Sillimanite

The analyses of five sillimanite prisms indicate that the mineral is of a nearly pure composition just like kyanite (Table 1).

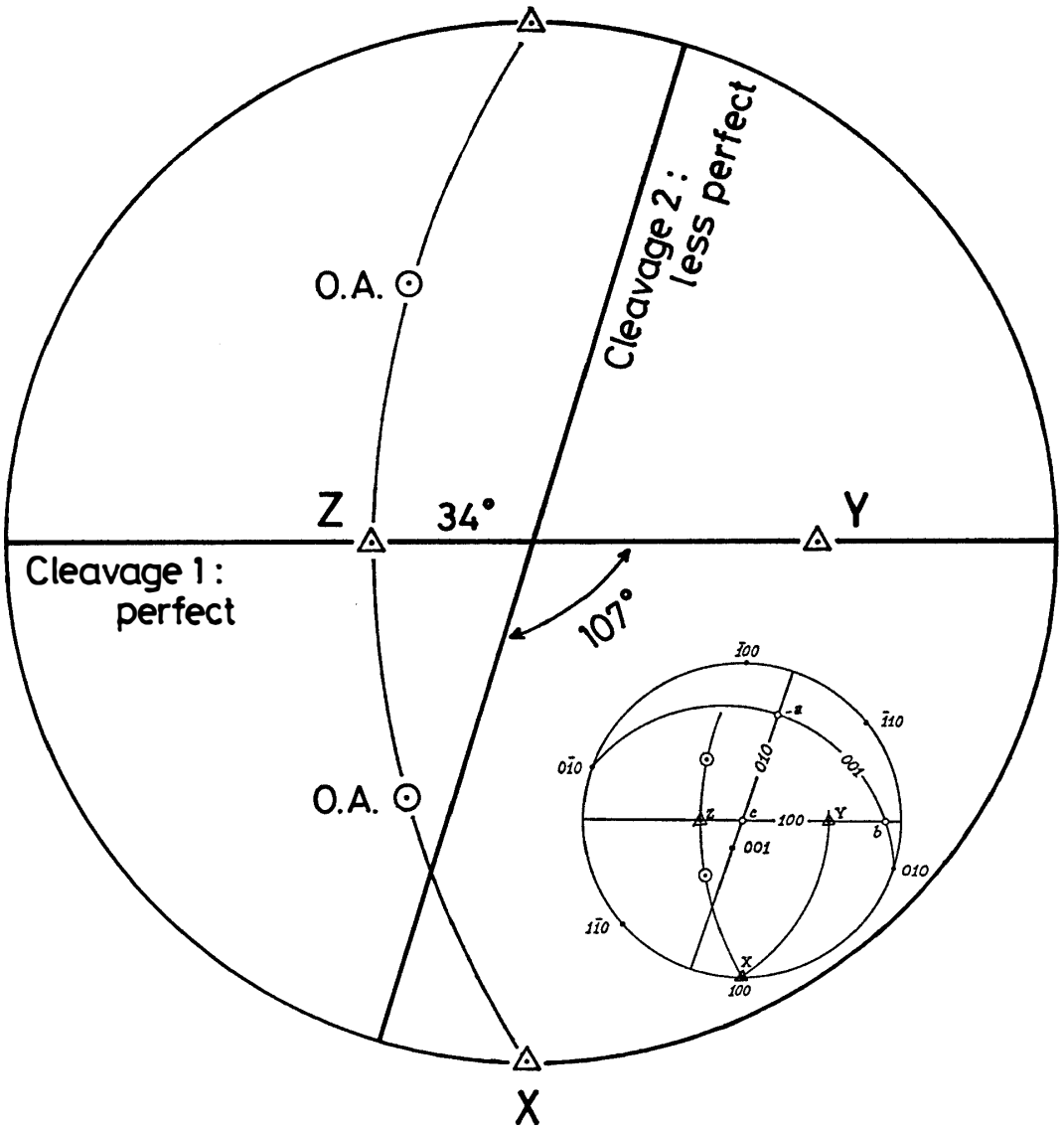

Fig. 4. Optical orientation of kyanite in the kyanite-bearing gneiss. The inset shows the kyanite orientation after PHILLIPS and GRIFFEN (1981).

4.3. Garnet

Garnet porphyroblasts are mostly idiomorphic to hypidiomorphic except for much embayed ones. Garnet compositions were determined on five porphyroblasts and some of them are listed in Table 2. Representative compositional profiles of three of the five porphyroblasts are illustrated in Figs. 5 and 6. A garnet (Ga_1) in Fig. 5 is shown in Fig. 2a. It has no marked embayed form but is only locally fringed by very minute flakes of Type-B biotite at the margin. Figure 5 shows a profile along the line A–B where the edge A is in contact with plagioclase and the edge B with the biotite (Fig. 2a). Two garnets (Ga_1^E and Ga_2^E) in Fig. 6 are shown in Fig. 2c. Figure 6 shows profiles along the lines C–D and E–F of the two garnets which are replaced by Type-B biotite at edges or along cracks. The edges C and D of Ga_1^E and the edge E of Ga_2^E are in contact with Type-B biotite. The edge F of Ga_2^E is adjacent to plagio-

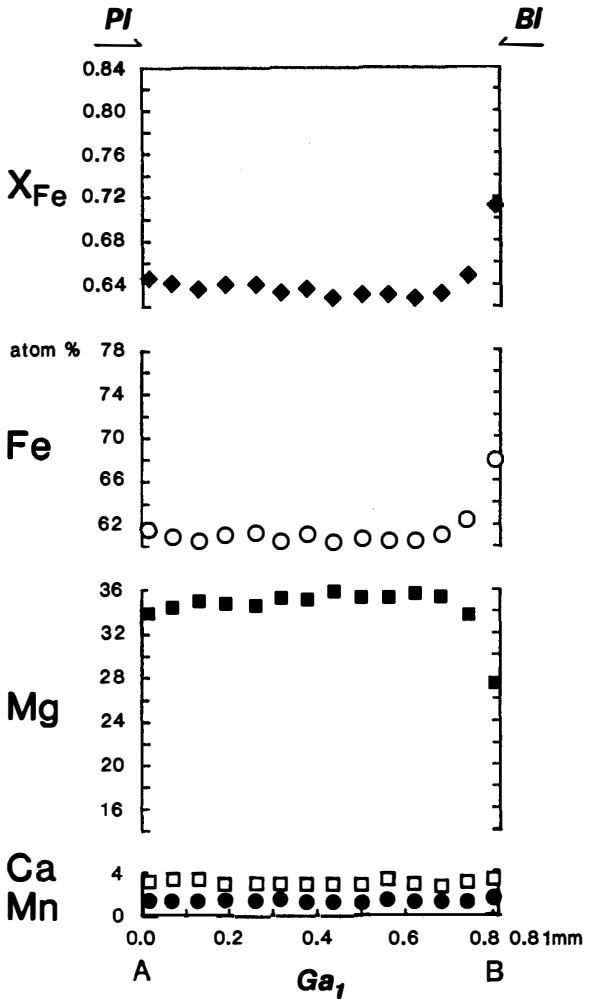

Fig. 5. Compositional profile of non-embayed garnet (Ga_1) along the line A–B in Fig. 2a.

clase, but films of Type-B biotite are developed along cracks near the edge F.

In both figures, the Ca and Mn contents are very low and almost uniform from one side to the other except for a slight increase of Mn near the contact with Type-B biotite. Thus garnet in this rock is close to that of almandine-pyrope series. In Fig. 5, Ga_1 is generally uniform in Fe and Mg contents and Fe/(Fe+Mg) ratio (X_{Fe}) and has magnesian compositions (X_{Fe}=0.63–0.65) from the interior to the edge A. However, Ga_1 shows an outward increase of X_{Fe} near the edge B, which results from an outward increase of the Fe content and a complementary decrease of the Mg content. Such an outward X_{Fe} increase is more striking in embayed Ga_1^E and Ga_2^E than in non-embayed Ga_1 (Fig. 6). It is noted in both figures that the interior compositions of embayed garnet, particularly Ga_2^E, are as magnesian as homogeneous compositions of non-embayed garnet (Ga_1).

The compositional uniformity within non-embayed garnet (Ga_1) suggests that sufficient atomic diffusion took place within the garnet and made the garnet to be homogeneous in composition. Such a condition would be easily realized during regional metamorphism of the amphibolite facies or of higher grade (BLACKBURN,

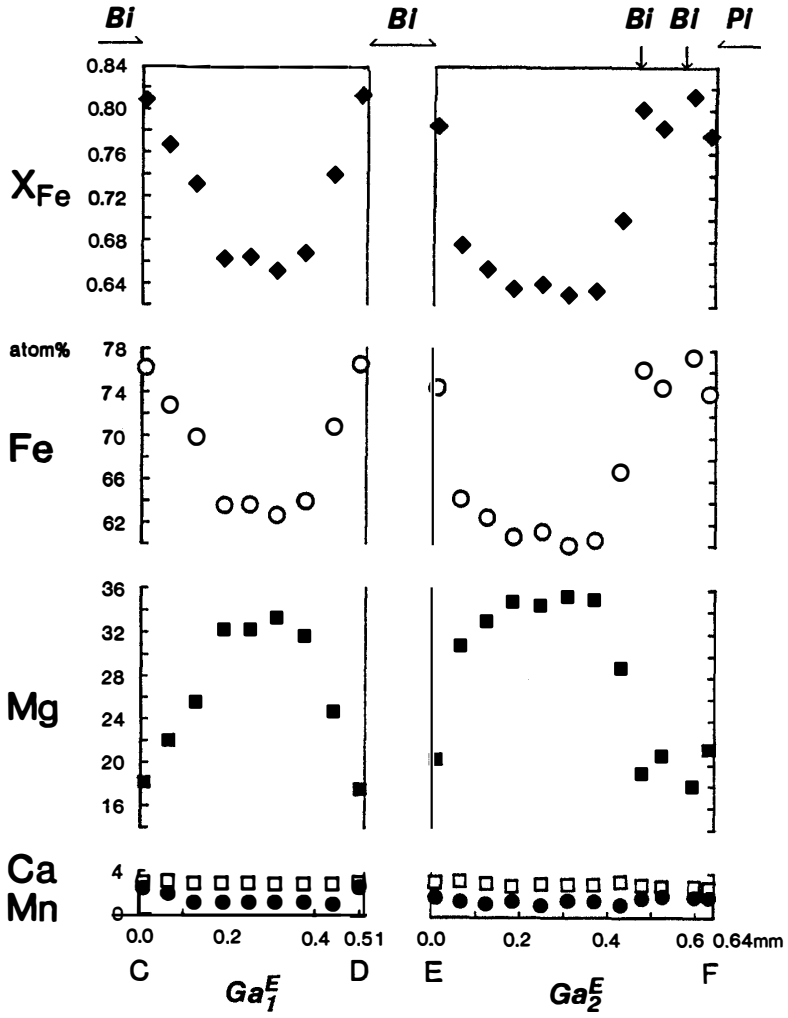

Fig. 6. Compositional profiles of embayed garnet (Ga_1^E and Ga_2^E) along the lines C–D and E–F in Fig. 2c.

1969; TRACY *et al.*, 1976; ANDERSON and OLIMPIO, 1977; WOODSWORTH, 1977; DIETVORST, 1982). Therefore, the homogeneous composition in Ga_1 is considered to have primarily been settled during the granulite-facies metamorphism in this area. On the other hand, the Fe-rich compositions at the edge may be ascribed to secondary modification by the formation of Type-B biotite.

4.4. Biotite

Type-A biotite shows pleochroism of X: pale yellow and $Y=Z$: reddish brown, while Type-B biotite does that of X: very pale yellow and $Y=Z$: yellowish brown to light brown. Corresponding to the differences of the mode of occurrence and pleochroism, the chemical compositions, especially the Ti content and X_{Fe}, are different between the two types. Analyses of many biotite flakes of two types are plotted on the Ti-X_{Fe} diagram (Fig. 7) and some of them are given in Table 3. Figure 7 displays that Type-A biotite is generally much higher in Ti content and similar to or little X_{Fe}-higher than Type-B biotite.

Type-B biotite analyzed is from two domains in this rock; one group is from

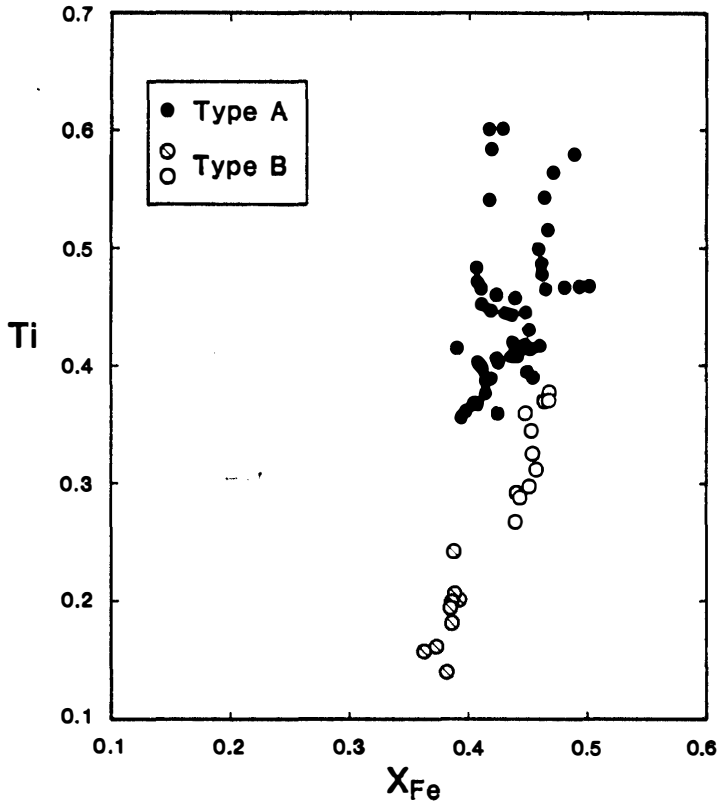

Fig. 7. Ti-X_{Fe} diagram of biotite. Type-B biotite is from two domains on the same thin section, the biotite from one domain (open circle) being distinguished in the diagram from that from the other domain (open circle with slash).

aggregates developed between Ga_1^E and Ga_2^E which are almost adjacent to each other as shown in Fig. 2c, and the other group is from those associated with another embayed garnet (Ga_3^E). Figure 7 also shows that the Ti content and X_{Fe} are somewhat different between the two groups.

4.5. Muscovite

Two muscovite flakes intimately associated with Type-B biotite and kyanite were analyzed. They are somewhat phengitic (Fe+Mg=0.23–0.28 based on O=22) and low in paragonite content (Pa_{5-6}) (Table 3).

4.6. Plagioclase

Plagioclase appears to be optically homogeneous among grains under the microscope. The microprobe analysis of six discrete grains in the matrix reveals that compositional zoning is actually absent or very weak with relatively albitic rim (An_{23-25}) to core (An_{24-26}) exemplified in Table 1.

4.7. K-feldspar

A perthitic texture of string type is often found in K-feldspar. Twelve, optically homogeneous or poorly perthitic grains were selected for analysis. Nevertheless, their orthoclase contents vary from 80 to 91 mol% among the grains. An analysis is representatively given in Table 1.

4.8. Spinel

Spinel is a light grayish green variety and occurs as minute allotriomorphic grains. Compositions of eight grains were determined. They are magnesian hercynite with a considerable amount of gahnite component (Table 1). Their compositions much vary among the grains: X_{Fe}=0.661–0.793 and ZnO=8.01–15.08 wt%.

4.9. Ilmenite and rutile

These minerals are of approximately pure compositions (Table 1).

5. Kyanite-Forming Reaction

The embayment of garnet by Type-B biotite accompanied by kyanite and quartz is characteristic in this rock as mentioned already. This textural relation may be well explained by the following garnet-consuming reaction:

$$\text{Garnet}+\text{K-feldspar}+H_2O=\text{Kyanite}+\text{Biotite}+\text{Quartz}\ . \qquad (1)$$

Garnet and K-feldspar on the left side represent the primary, granulite-facies association and the three minerals on the right side do the secondary, hydrated or retrograde assemblage. The reaction is further supported by the following two lines of evidence.

One is the change of Mn content at the embayed garnet edge. Mn is much more concentrated in garnet than in biotite (ALBEE, 1972; THOMPSON, 1976a). It is expected from this relation that Mn is enriched near the embayed edge, if atomic diffusion within garnet is insufficient during its partial replacement by biotite. In the present case, Mn-enrichment is obviously recognized at the well-embayed edge though its degree is low (Fig. 6), suggesting partial replacement of the garnet by Type-B biotite.

The other is paragenetic relationships among kyanite, biotite, garnet and K-feldspar. Mineral parageneses involving these minerals and muscovite in this rock can be approximately represented in the four-component system Al_2O_3-K_2O-FeO-MgO with excess quartz, provided that H_2O is a perfect mobile component. Firstly, the association of garnet (interior) and K-feldspar and that of kyanite and Type-B biotite are shown in the A′KF′ diagram (Fig. 8). The two tie-lines intersect with each other, so that the reaction relation holds good in this diagram. As already stated, the minerals kyanite, embayed garnet edge and Type-B biotite coexist with not only quartz but also muscovite. Secondly, two sets of the association of kyanite, garnet (embayed edge) and Type-B biotite are depicted in the AFM diagram together with corresponding two sets of the garnet interior composition (Fig. 9). The two sets are from the two different domains within this rock. Although the primary garnet represented by the magnesian garnet interior, like Ga_1 in Fig. 5, coexists with K-feldspar and thus their association is not represented on the AFM diagram which was projected from muscovite onto the AFM plane (THOMPSON, 1957), the garnet compositions are plotted on Fig. 9 for examining the compositional relation to the secondary three-phase assemblage. Figure 9 exhibits that the interior composition lies in the three-phase field formed by the association kyanite-garnet (edge)-biotite (Type B) in either of the two sets. Such a relationship suggests that the primary garnet broke down to produce kyanite and type-B biotite and to change the composition toward the Fe-rich

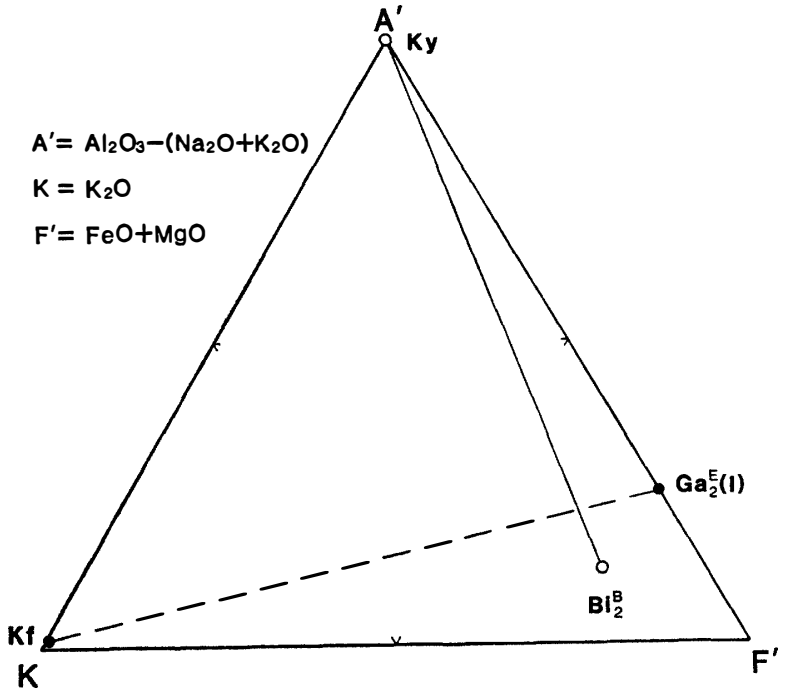

Fig. 8. A'KF' diagram showing a paragenetic relation between the associations garnet (interior)-K-feldspar and kyanite-Type-B biotite. The compositions of $Ga_2^E(I)$ and Bi_2^B in Tables 2 and 3 are plotted as representative values of embayed-garnet interior and Type-B biotite.

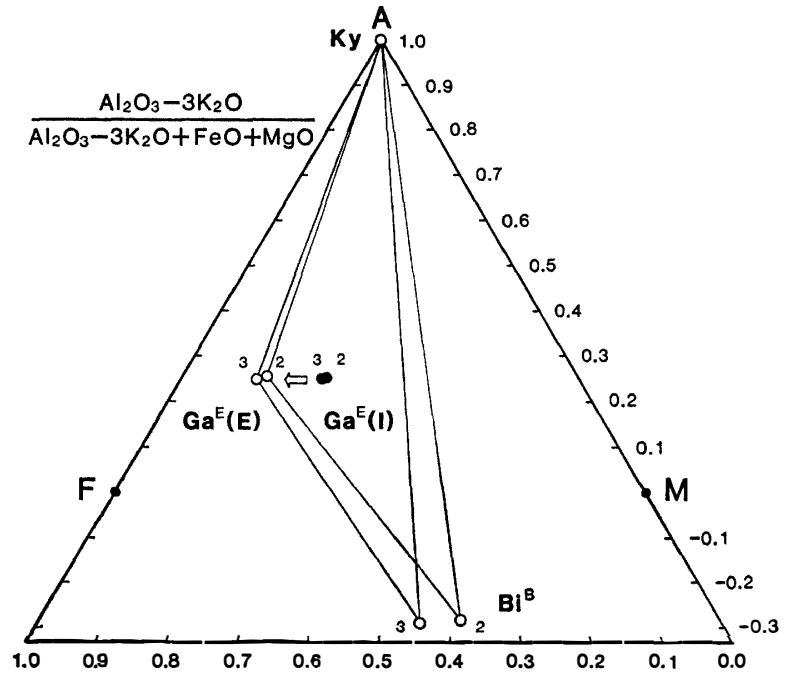

Fig. 9. AFM diagram showing a paragenetic relation between the associations kyanite-garnet (embayed edge)-Type-B biotite and garnet (interior). (I): garnet interior, (E): garnet edge. The numbers 2 and 3 refer to Ga_2^E and Ga_3^E in Table 2 and Bi_2^B and Bi_3^B in Table 3, respectively. $Ga_2^E(E)$ and $Ga_3^E(E)$ are in contact with Bi_2^B and Bi_3^B, respectively.

side at the same time.

In conclusion, it is highly probable that kyanite was formed through the retrograde reaction (1).

Muscovite is also associated exclusively with Type-B biotite but aggregates composed of both micas sometimes lack kyanite as shown in Fig. 2b. Such relations suggest that the embayment of garnet is also due to another garnet-consuming reaction:

$$\text{Garnet}+\text{K-feldspar}+H_2O=\text{Biotite}+\text{Muscovite}+\text{Quartz}\ . \qquad (2)$$

Therefore, the coupled reaction of the reactions (1) and (2) may also be responsible for the retrograde development of kyanite.

6. Physical Conditions of Metamorphism

On the basis of the characteristic textural and paragenetic relations, minerals in this rock may be grouped into the following two kinds of mineral assemblages of different stage and grade.

(1) Granulite-facies one (with ilmenite and rutile):
   (a) sillimanite+magnesian garnet+Type-A biotite+K-feldspar+plagioclase+quartz.
   (b) spinel+sillimanite+magnesian garnet+Type-A biotite+plagioclase.

(2) Retrograde one:
   kyanite+Fe-rich garnet+Type-B biotite+muscovite+quartz.

The magnesian garnet corresponds to the non-embayed garnet of homogeneous composition and the interior of embayed garnet, whereas the Fe-rich garnet does to the embayed garnet edge.

Metamorphic temperatures of the both stages were estimated from compositions of garnet-biotite pairs according to THOMPSON (1976b). Compositions used are from the garnet interior and Type-A biotite, the latter of which is present near the garnet

Table 4. Garnet-biotite thermometry and garnet-plagioclase barometry.

84021904B	$(Mg/Fe)^{Ga}$	$(Mg/Fe)^{Bi}$	K_D^{Bi-Ga}	X_{Gr}	X_{An}	T_T (°C)	P_{NH} (kb) (at 830°C)
Ga_1(I)-Bi_1^A-Pl_1(C)	0.580	1.507	2.597	0.029	0.261	819	7.8
Ga_2(I)-Bi_2^A-Pl_2(C)	0.573	1.407	2.454	0.028	0.255	844	7.9
Ga_2^E(I)-Bi_3^A-Pl_3(C)	0.572	1.445	2.525	0.029	0.243	832	8.3
Ga_3^E(I)-Bi_4^A	0.551	1.382	2.508	0.027		835	
Ga_2^E(E)-Bi_2^B	0.274	1.626	5.934	0.032		550	
Ga_3^E(E)-Bi_3^B	0.238	1.263	5.304	0.030		579	
Ga_4^E(E)-Bi_4^B	0.216	1.199	5.543	0.031		568	
Ga_5^E(E)-Bi_5^B	0.201	1.252	6.231	0.032		539	

Ga: non-embayed garnet, Ga^E: embayed garnet, (I): interior, (E): edge, Bi^A: Type-A biotite, Bi^B: Type-B biotite, (C): core.

T_T: after THOMPSON (1976b), P_{NH}: after NEWTON and HASELTON (1981).

All the compositions of garnet, biotite and plagioclase listed above are included in Tables 1 to 3.

concerned, for estimating the granulite-facies temperatures. The others are from the embayed garnet edge and Type-B biotite contacting with the edge for estimating the retrograde ones. Data on four garnet-biotite pairs in each grade are available. Their results are given in Table 4. 820–840°C and 540–580°C are obtained as the granulite-facies and the retrograde temperatures, respectively. Metamorphic solid pressures of the granulite-facies are calculated by the method of NEWTON and HASELTON (1981) from compositions of the garnet interior and the core of plagioclase contacting with the garnet. Three pairs available give 7.8–8.3 kb (Table 4). Pressure estimate of the retrograde stage by means of this mineral pair is impossible at present, because no plagioclase adjacent to the embayed garnet edge has yet been found.

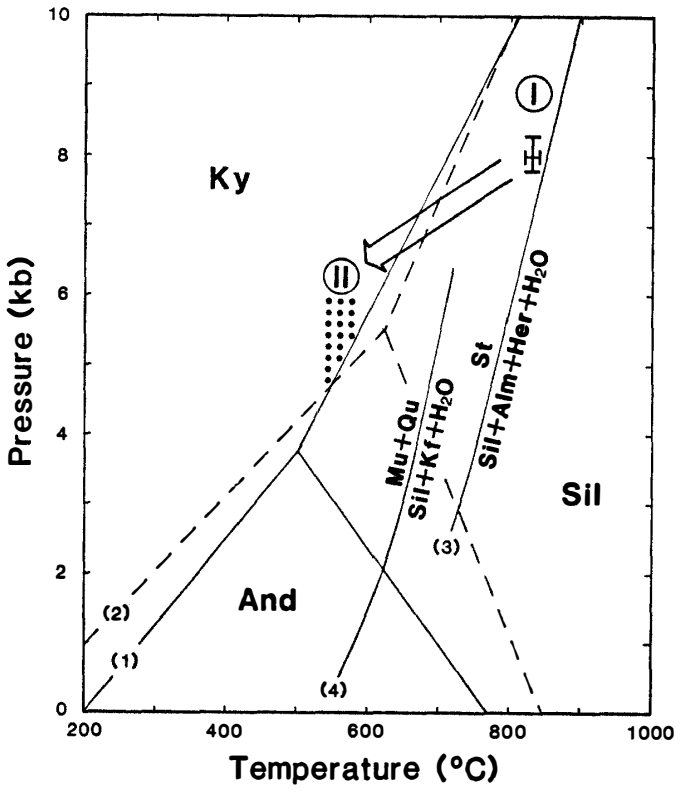

Fig. 10. Estimated T-P conditions of the granulite-facies metamorphism (I) and retrograde one (II). (1) HOLDAWAY (1971), (2) RICHARDSON et al. (1969), (3) RICHARDSON (1968) and (4) CHATTERJEE and JOHANNES (1974). Mineral abbreviations: Alm, almandine; And, andalusite; Her, hercynite; Kf, K-feldspar; Ky, kyanite; Mu, muscovite; Qu, quartz; Sil, sillimanite; St, staurolite.

A range of the granulite-facies conditions obtained are located in a *P-T* diagram with some univariant reaction curves (Fig. 10). The conditions are consistent with those inferred from the sillimanite-K-feldspar association which is stable within the stability field of sillimanite and beyond that of muscovite plus quartz at the same time. The association spinel-sillimanite-garnet (-H_2O) is chemically equivalent to staurolite in the Al_2O_3-FeO-SiO_2-H_2O system and is stable on higher temperature side than the latter (RICHARDSON, 1968). In Fig. 10, the *T-P* range obtained from this rock is a little lower in temperature than Richardson's staurolite-breakdown curve. However, this inconsistency seems to be apparent for two reasons. First, the position of the curve is not necessarily exact, because it is an estimated one based on a metastable staurolite-breakdown reaction investigated experimentally (RICHARDSON, 1966, 1968). Second, the breakdown temperatures of staurolite would be lowered if the ZnO com-

ponent is added in the above system. In fact, spinel in this rock is rich in ZnO (Table 1). Therefore, the *T-P* range in Fig. 10 is also a probable one in connection with the staurolite-breakdown reaction, even though the position of the reaction curve is certain in *T-P* plot. Moreover, this range is in good agreement with the *T-P* estimates (about 800°C and 7–8.5 kb) which were independently obtained from compositions of some minerals in the basic to intermediate rocks from the same granulite-facies terrane (SHIRAISHI and KOJIMA, 1987).

The granulite-facies metamorphism in this area is likely to differ in baric type from that of low pressure in the Yamato Mountains about 300 km east of this area (ASAMI and SHIRAISHI, 1985). In this respect, the metamorphism in this area is similar to that of medium pressure in the Prince Olav Coast to Lützow-Holm Bay region 300 km or further northeast of the Yamato Mountains (HIROI *et al.*, 1983a, b; MOTOYOSHI *et al.*, 1985; MOTOYOSHI and SHIRAISHI, 1985; KATSUSHIMA, 1985).

The retrograde metamorphic conditions should be in a *T-P* field where the kyanite field overlaps the muscovite-quartz field. Adopting 540–580°C as the retrograde metamorphic temperatures, the kyanite-andalusite and kyanite-sillimanite equilibrium curves after RICHARDSON *et al.* (1969) and HOLDAWAY (1971) give the retrograde pressures higher than 4.5 kb (Fig. 10). Taking the medium-pressure character of the granulite-facies metamorphism into consideration, the retograde metamorphic event would have taken place either at the later stage of the granulite-facies regional one during uplifting or as a result of reheating by acid magma intruded in this area at a somewhat deep crustal level during or after the uplift. A possible retrograde-metamorphic *P-T-t* path is shown as the simplest case in Fig. 10. It is noteworthy that such a path is much different from that known in the Prince Olav Coast to Lützow-Holm Bay region (HIROI *et al.*, 1984), where andalusite widely occurs as a retrograde mineral of contact metamorphic origin (HIROI *et al.*, 1983a, b). Unlike the western part of the Sør Rondane Mountains, retrograde andalusite and cordierite are found in the central part (YAMAZAKI *et al.*, 1986; ISHIZUKA and KOJIMA, 1987). However, the genetic relationship of retrograde metamorphic events between the two areas remains uncertain at present.

Acknowledgments

We would like to express our sincere thanks to Mr. H. KOJIMA of National Institute of Polar Research and Dr. Y. MOTOYOSHI of the University of New South Wales for their kind help during microprobe analyses. One of us (M. A.) is indebted to Prof. T. NUREKI and Dr. SHIBATA of Okayama University for their critical discussion. Thanks are also due to Miss K. SHIMAOKA of Okayama University for preparing the manuscript.

References

ALBEE, A. L. (1972): Metamorphism of pelitic schists; Reaction relations of chloritoid and staurolite. Geol. Soc. Am. Bull., **83**, 3249–3268.

ANDERSON, D. E. and OLIMPIO, J. C. (1977): Progressive homogenization of metamorphic garnets,

South Morar, Scotland; Evidence for volume diffusion. Can. Mineral., **15**, 205–216.

ASAMI, M. and SHIRAISHI, K. (1985): Retrograde metamorphism in the Yamato Mountains, East Antarctica. Mem. Natl Inst. Polar Res., Spec. Issue, **37**, 147–163.

BLACKBURN, W. H. (1969): Zoned and unzoned garnets from the Grenvile gneisses around Gananoque, Ontario. Can. Mineral., **9**, 691–698.

CHATTERJEE, N. D. and JOHANNES, W. (1974): Thermal stability and standard thermodynamic properties of synthetic $2M_1$-muscovite, $KAl_2[AlSi_3O_{10}(OH)_2]$. Contrib. Mineral. Petrol., **48**, 89–114.

DIETVORST, E. J. L. (1982): Retrograde garnet zoning at low water pressure in metapelitic rocks from Kemiö, SW Finland. Contrib. Mineral. Petrol., **79**, 37–45.

HIROI, Y., SHIRAISHI, K., YANAI, K. and KIZAKI, K. (1983a): Aluminum silicates in the Prince Olav and Sôya Coasts, East Antarctica. Mem. Natl Inst. Polar Res., Spec. Issue, **28**, 115–131.

HIROI, Y., SHIRAISHI, K., NAKAI, Y., KANO, T. and YOSHIKURA, S. (1983b): Geology and petrology of Prince Olav Coast, East Antarctica. Antarctic Earth Science, ed. by R. L. OLIVER *et al.* Canberra, Aust. Acad. Sci., 32–35.

HIROI, Y., SHIRAISHI, K., MOTOYOSHI, Y. and YANAI, K. (1984): Syowa Kiti shûhen ni bunpu suru genseidai henseiganrui no keisei ni taisuru purêto tekutonikku moderu (Plate tectonic model of the development of the Proterozoic metamorphics in the area around Syowa Station). Dai-5-kai Nankyoku Chigaku Shinpojiumu Puroguramu·Kôen Yôshi (Program·Abstr. 5th Symp. Antarct. Geosci.). Tokyo, Natl Inst. Polar Res., 42–43.

HOLDAWAY, M. J. (1971): Stability of andalusite and the aluminum silicate phase diagram. Am. J. Sci., **271**, 97–131.

ISHIZUKA, H. and KOJIMA, H. (1987): A preliminary report on the geology of the central part of the Sør Rondane Mountains, East Antarctica. Proc. NIPR Symp. Antarct. Geosci., **1**, 113–128.

KATSUSHIMA, T. (1985): Granulite-facies rocks in several islands west of Langhovde, East Antarctica. Mem. Natl Inst. Polar Res., Spec. Issue, **37**, 95–110.

KOJIMA, S. and SHIRAISHI, K. (1986): Note on the geology of the western part of the Sør Rondane Mountains, East Antarctica. Mem. Natl Inst. Polar Res., Spec. Issue, **43**, 116–131.

MOTOYOSHI, Y. and SHIRAISHI, K. (1985): Petrography and geothermometry-geobarometry of Botnnuten, East Antarctica. Mem. Natl Inst. Polar Res., Spec. Issue, **37**, 127–146.

MOTOYOSHI, Y., MATSUBARA, S., MATSUEDA, H. and MATSUMOTO, Y. (1985): Garnet-sillimanite gneisses from the Lützow-Holm Bay region, East Antarctica. Mem. Natl Inst. Polar Res., Spec. Issue, **37**, 82–94.

NEWTON, R. C. and HASELTON, H. J. (1981): Thermodynamics of the garnet-plagioclase-Al_2SiO_5-quartz geobarometer. Thermodynamics of Minerals and Melts, ed. by R. C. NEWTON *et al.* New York, Springer, 125–145.

PHILLIPS, W. R. and GRIFFEN, D. T. (1981): Optical Mineralogy. San Francisco, Freeman.

RICHARDSON, S. W. (1966): Staurolite. Carnegie Inst. Washington, Yearb., **65**, 248–252.

RICHARDSON, S. W. (1968): Staurolite stability in a part of the system Fe-Al-Si-O-H. J. Petrol., **9**, 467–488.

RICHARDSON, S. W., GILBERT, M. C. and BELL, P. M. (1969): Experimental determination of kyanite-andalusite and andalusite-sillimanite equilibria; The aluminum silicate triple point. Am. J. Sci., **267**, 259–272.

SHIRAISHI, K. and KOJIMA, S. (1987): Basic and intermediate gneisses from the western part of the Sør Rondane Mountains, East Antarctica. Proc. NIPR Symp. Antarct. Geosci., **1**, 129–149.

THOMPSON, A. B. (1976a): Mineral reactions in pelitic rocks; I. Prediction of P-T-X (Fe-Mg) phase relations. Am. J. Sci., **276**, 401–424.

THOMPSON, A. B. (1976b): Mineral reactions in pelitic rocks; II. Calculation of some P-T-X (Fe-Mg) phase relations. Am. J. Sci., **276**, 425–454.

THOMPSON, J. B. (1957): The graphical analysis of mineral assemblages in pelitic schists. Am. Mineral., **42**, 842–858.

TRACY, R. J., ROBINSON, P. and THOMPSON, A. B. (1976): Garnet composition and zoning in the

determination of temperature and pressure of metamorphism, central Massachusetts. Am. Mineral., **61**, 762–775.

WOODSWORTH, G. J. (1977): Homogenization of zoned garnets from pelitic schists. Can. Mineral., **15**, 230–242.

YAMAZAKI, M., YOSHIKURA, S., ISHIZUKA, H. and KOJIMA, H. (1986): Sêru Rondâne Sanchi no henseigan to henseisayô (Metamorphic rocks and metamorphism in the Sør Rondane Mountains). Dai-7-kai Nankyoku Chigaku Shinpojiumu Purogramu·Kôen Yôshi (Program·Abstr. 7th Symp. Antarct. Geosci.). Tokyo, Natl Inst. Polar Res., 44–45.

(Received April 6, 1987; Revised manuscript received May 25, 1987)